A Position Sensorless Induction Machine Drive For Electric Vehicle Applications

C. J. Bonanno *Student Member, IEEE*
Li Zhen *Student Member, IEEE*
Dr. Longya Xu *Senior Member, IEEE*

The Center for Automotive Research - Department of Electrical Engineering
The Ohio State University
2015 Neil Avenue
Columbus, Ohio 43210

Abstract- The rotor speed is estimated for a position sensorless induction machine drive using a physical approach. This physical approach uses a frequency compensation scheme to estimate the rotor flux accurately at low speeds and subject to parameter variations. After background material is presented to explain the principles of the estimator, a computer simulation is conducted of a field oriented drive with the estimator. Based on the favorable results of the simulation, a laboratory investigation is conducted of the proposed drive.

I. Introduction

The development of cost effective, long distance electric vehicles is close to realization. However, the type of electric machine that should be used in future electric vehicles is still a debated subject. Switched reluctance machines have several advantages, and have many features that are quite suited for EVs. The cage rotor or doubly fed induction machine still has several noteworthy advantages, however, including field weakening, tough and rugged construction, low cost, and simplified inverter/machine interface. The *sensorless* operation of an induction machine is attractive for electric vehicle applications because of increased reliability, decreased overall cost, and a less restrictive geometry for the drive. Finally, in the theme of *packaging,* the physical approach algorithm is easily incorporated into a dedicated hardware system.

Many sensorless drives have been developed using different approaches. A physical approach was taken in [1], while more control oriented approaches were taken in [2],[3]. In [1], the authors presented a rotor flux oriented, position sensorless induction machine drive and showed that if the normal integration process is used to calculate the rotor flux, changing parameter values and low speed effects will result in an incorrect estimate. An inaccurate rotor flux estimate, in turn, produces an incorrect rotor speed estimate. The authors of [1] proposed a solution in which simple low pass filtering of both the back emf and flux command is done, resulting in a robust flux estimator which is largely insensitive to parameter variations and works well in a low speed range. In [2], the authors used the difference between two flux estimators and proposed a novel pole assignment method to realize a robust flux observer. This approach is more of a control oriented approach because of the use of Popov's criteria, linearization, and state-space pole assignment. There is less emphasis on machine physics, and how the machine physics affect rotor flux estimation. In [3], adaptive control theory is applied to synthesize an estimator. In addition, the estimator uses a parameter adaptive scheme to compensate for changing parameter values. For these reasons, we classify the approach in [3] as control oriented as well.

Two principle advantages exist in developing a drive using the approach of [1]. One, there is essentially no control system design needed to produce the flux estimator. No time is required to tune the estimator. For the physical approach, the critical information needed for implementation is the value of the rotor time constant. Two, the estimation algorithm is easily implemented in a DSP or dedicated hardware.

Rotor field orientation is reviewed, and the system structure for the rotor flux estimator is presented. The speed estimator scheme is discussed. The accuracy of the estimator is first tested on a indirect field oriented drive, and then a laboratory investigation is conducted of the proposed estimation scheme.

II. Rotor Field Orientation

A. *Machine Model*

The synchronous frame, rotor flux oriented d-q induction machine model is shown in Figure 1.

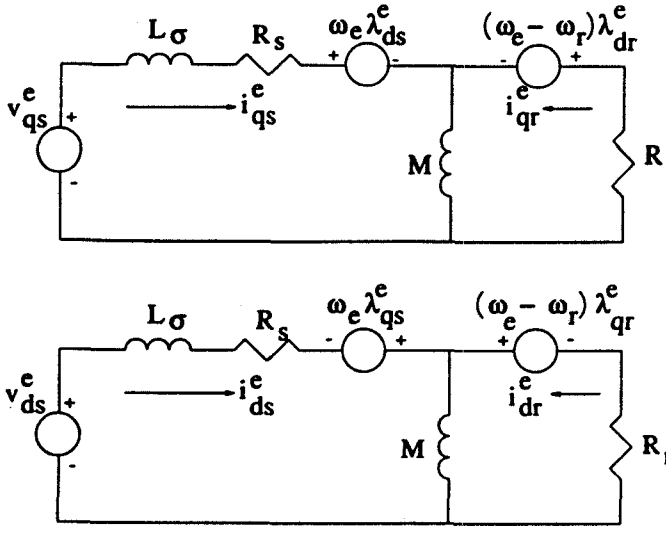

Figure 1: Rotor Flux d-q Model

The fifth order set of differential equations which describe a three phase symmetrical induction machine are:

$$v^e_{qs} = L_\sigma \frac{di^e_{qs}}{dt} + R_s i^e_{qs} + \omega_e \lambda^e_{ds} + \frac{d\lambda^e_{qr}}{dt} \quad (1)$$

$$v^e_{ds} = L_\sigma \frac{di^e_{ds}}{dt} + R_s i^e_{ds} - \omega_e \lambda^e_{qs} + \frac{d\lambda^e_{dr}}{dt} \quad (2)$$

$$v^e_{qr} = R_r i^e_{qr} + (\omega_e - \omega_r)\lambda^e_{dr} + \frac{d\lambda^e_{qr}}{dt} \quad (3)$$

$$v^e_{dr} = R_r i^e_{dr} - (\omega_e - \omega_r)\lambda^e_{qr} + \frac{d\lambda^e_{dr}}{dt} \quad (4)$$

$$T_e = J\frac{d\omega_{rm}}{dt} + B_m\omega_{rm} + T_l \quad (5)$$

where

$$\lambda^e_{qr} = M(i^e_{qs} + i^e_{qr}) \quad (6)$$

$$\lambda^e_{dr} = M(i^e_{ds} + i^e_{dr}) \quad (7)$$

$$T_e = \frac{3P}{4}(\lambda^e_{dr} i^e_{qs} - \lambda^e_{qr} i^e_{ds}) \quad (8)$$

The first principle of field orientation is to align the rotor flux with the d axis. This forces $\lambda^e_{qr} = 0$. The conditions for field orientation control are derived from the rotor voltage and rotor flux equations listed above, with the condition $\lambda^e_{qr} = 0$. Equations (3) (4) (6) (7) and (8) are listed in reduced form:

$$(\omega_e - \omega_r) = \frac{-R_r i^e_{qr}}{\lambda^e_{dr}} \quad (9)$$

$$\frac{d\lambda^e_{dr}}{dt} = -R_r i^e_{dr} \quad (10)$$

$$i^e_{qs} = -i^e_{qr} \quad (11)$$

$$\lambda^e_{dr} = M(i^e_{ds} + i^e_{dr}) \quad (12)$$

$$T_e = \frac{3P}{4}(\lambda^e_{dr} i^e_{qs}) \quad (13)$$

The slip condition is found by inserting (11) into (9);

$$\omega_e - \omega_r = s\omega_e = \frac{R_r i^e_{qs}}{\lambda^e_{dr}} \quad (14)$$

From Equation (12),

$$i^e_{dr} = \frac{\lambda^e_{dr}}{M} - i^e_{ds} \quad (15)$$

The flux condition is found by inserting (15) into (10);

$$\lambda^e_{dr} = \frac{M i^e_{ds}}{1 + T_r p} \quad (16)$$

where T_r is the rotor time constant and is equal to

$$T_r = \frac{M}{R_r} \quad (17)$$

B. *Rotor Flux Estimation Scheme*

The stationary frame *vector* model of the rotor flux oriented induction machine is shown in Figure 2. This model is chosen because it is the basis for rotor flux estimation. The block diagram of the proposed rotor flux estimator is shown in Figure 3.

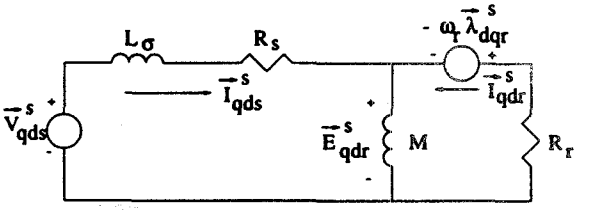

Figure 2: Vector Model in Stationary Frame

Note that the block diagram realizes the rotor flux estimator according to the following equation:

$$\vec{\lambda}^s_{qdr} = \frac{T_c \vec{E}^s_c}{1 + T_c p} + \frac{\vec{\lambda}^{s^*}_{qdr}}{1 + T_c p} \quad (18)$$

The frequency domain version of (18) is:

$$\vec{\lambda}^s_{qdr} = \frac{T_c \vec{E}^s_c}{1 + j\omega_e T_c} + \frac{\vec{\lambda}^{s^*}_{qdr}}{1 + j\omega_e T_c} \quad (19)$$

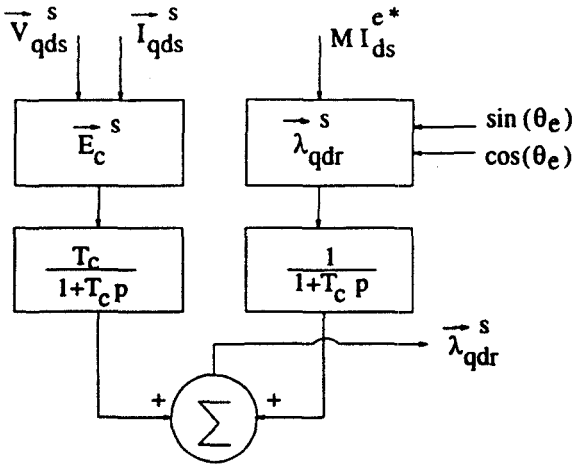

Figure 3: Flux Estimator Block Diagram

where the vectors are defined as:

$$\vec{\lambda}^{s^*}_{qdr} = \begin{bmatrix} \lambda^{s^*}_{qr} \\ \lambda^{s^*}_{dr} \end{bmatrix} \vec{E}^{s}_{c} = \begin{bmatrix} E^{s}_{cqr} \\ E^{s}_{cdr} \end{bmatrix} \vec{\lambda}^{s}_{qdr} = \begin{bmatrix} \lambda^{s}_{qr} \\ \lambda^{s}_{dr} \end{bmatrix} \tag{20}$$

Using the stator voltages and currents, the calculated back emf, $\vec{E}^{s}_{c}$, is given by:

$$\vec{E}^{s}_{c} = \vec{V}^{s}_{qds} - (R^{*}_{s} + j\omega_e L^{*}_{\sigma})\vec{I}^{s}_{qds} \tag{21}$$

where R^{*}_{s} and L^{*}_{σ} are the nominal values of stator resistance and leakage inductance. The nominal values are related to the actual values by:

$$R^{*}_{s} = R_s - \Delta R_s \tag{22}$$

$$L^{*}_{\sigma} = L_\sigma - \Delta L_\sigma \tag{23}$$

Inserting (22) and (23) into (21) yields:

$$\vec{E}^{s}_{c} = \vec{V}^{s}_{qds} - ((R_s - \Delta R_s) + j\omega_e(L_\sigma - \Delta L_\sigma))\vec{I}^{s}_{qds} \tag{24}$$

According to Figure 2, the actual back emf, $\vec{E}^{s}_{qdr}$, is

$$\vec{E}^{s}_{qdr} = \vec{V}^{s}_{qds} - (R_s + j\omega_e L_\sigma)\vec{I}^{s}_{qds} \tag{25}$$

Therefore, the calculated and actual back emfs are related by

$$\vec{E}^{s}_{c} = \vec{E}^{s}_{qdr} + (\Delta R_s + j\omega_e \Delta L_\sigma)\vec{I}^{s}_{qds} \tag{26}$$

For notation purposes, the following expressions are introduced:

$$\vec{\mu} = \frac{1}{1 + j\omega_e T_c} = |\vec{\mu}|\, \angle\phi \tag{27}$$

where

$$|\vec{\mu}| = \frac{1}{\sqrt{1+(\omega_e T_c)^2}} \quad \text{and} \quad \angle\phi = -tan^{-1}(\omega_e T_c) \tag{28}$$

Then, the estimated flux expressed in (19) becomes:

$$\vec{\lambda}^{s}_{qdr} = \vec{\mu}\, T_c\, \vec{E}^{s}_{c} + \vec{\mu}\, \vec{\lambda}^{s^*}_{qdr} \tag{29}$$

The torque current i^{e}_{qs} in the synchronous reference frame is estimated from the stationary flux components by:

$$i^{e}_{qs} = \frac{i^{s}_{qs}\lambda^{s}_{dr} - i^{s}_{ds}\lambda^{s}_{qr}}{\sqrt{(\lambda^{s}_{dr})^2 + (\lambda^{s}_{qr})^2}} \tag{30}$$

C. *Speed Estimation Scheme*

The slip speed and synchronous speed can be calculated from the estimated rotor flux. It follows that the estimated rotor speed is the difference between the synchronous and slip speeds. The slip speed $s\,\omega_e$ in a rotor flux oriented drive is *uniquely* determined by the torque current i^{e}_{qs} and rotor flux magnitude $|\lambda^{e}_{dr}|$,

$$s\,\omega_e = \frac{R_r\, i^{e}_{qs}}{|\lambda^{e}_{dr}|} \tag{31}$$

with i^{e}_{qs} obtained from Equation (30), and the magnitude of the rotor flux obtained through:

$$|\lambda^{e}_{dr}| = \sqrt{(\lambda^{s}_{dr})^2 + (\lambda^{s}_{qr})^2} \tag{32}$$

The synchronous speed is also estimated from the rotor flux:

$$\omega_e = \frac{\lambda^{s}_{qr}\lambda^{s}_{dr} - \lambda^{s}_{qr}\lambda^{s}_{dr}}{(\lambda^{s}_{dr})^2 + (\lambda^{s}_{qr})^2} \tag{33}$$

The rotor speed, therefore, is

$$\omega_{rm} = \omega_e - s\,\omega_e \tag{34}$$

D. *Parameter Sensitivity and Low Speed Effects*

In order to investigate the parameter sensitivity and low speed effects of the proposed estimation scheme, Equations (26) and (29) are combined to form:

$$\vec{\lambda}^{s}_{qdr} = \vec{\mu}\, T_c(\vec{E}^{s}_{qdr} + (\Delta R_s + j\omega_e \Delta L_\sigma)\, \vec{I}^{s}_{qds}) + \vec{\mu}\, \vec{\lambda}^{s^*}_{qdr} \tag{35}$$

Let

$$\vec{\lambda}^{s}_{qdr} = \vec{\lambda}_1 + \vec{\lambda}_2 + \vec{\lambda}_3 \tag{36}$$

Then

$$\vec{\lambda}_1 = \vec{\mu}\, T_c\, \vec{E}^{s}_{qdr} \tag{37}$$

$$\vec{\lambda}_2 = \vec{\mu}\, T_c\, (\Delta R_s + j\omega_e \Delta L_\sigma)\, \vec{I}^{s}_{qds} \tag{38}$$

$$\vec{\lambda}_3 = \vec{\mu}\, \vec{\lambda}^{s^*}_{qdr} \tag{39}$$

1. Parameter Sensitivity

It is observed that only $\vec{\lambda}_2$ is subjected to parameter variations, and thus the robustness of the estimator will improve if $\vec{\lambda}_2$ is negligibly small. The vector $\vec{\lambda}_2$ can be made to approximate zero by a proper selection of T_c, the filter time constant. To examine this, Equation (38) is re-written as:

$$\vec{\lambda}_2 = \vec{\mu}\, T_c\, \Delta Z \angle\gamma\, \vec{I}^s_{qds} \tag{40}$$

where

$$\Delta Z = \sqrt{\Delta R_s{}^2 + (\omega_e \Delta L_\sigma)^2} \tag{41}$$

and

$$\gamma = tan^{-1}\left(\frac{\omega_e \Delta L_\sigma}{\Delta R_s}\right) \tag{42}$$

Equation (40) can also be expressed as:

$$\vec{\lambda}_2 = T_c |\vec{\mu}| \Delta Z \angle(\phi + \gamma) \vec{I}^s_{qds} \tag{43}$$

Setting $\phi + \gamma = 0$,

$$tan^{-1}(\omega_e T_c) = tan^{-1}\left(\frac{\omega_e \Delta L_\sigma}{\Delta R_s}\right) \tag{44}$$

This requires that

$$T_c = \frac{\Delta L_\sigma}{\Delta R_s} \tag{45}$$

Note that

$$\frac{\Delta L_\sigma}{\Delta R_s} \doteq \frac{M}{R_r} \tag{46}$$

Thus, by choosing

$$T_c = \frac{M}{R_r} \tag{47}$$

which is exactly the rotor time constant, the phase of $\vec{\lambda}_2$ will be approximately zero. Likewise,

$$\Delta Z |\vec{\mu}| = 1 \tag{48}$$

Equation (43) can be written as:

$$\vec{\lambda}_2 = T_c \vec{I}^s_{qds} \tag{49}$$

As indicated, parameter sensitivity is minimized by minimizing $\vec{\lambda}_2$ in terms of both magnitude and phase angle.

2. Low Speed Effects

The performance improvement of the flux estimator is explained by examining $\vec{\lambda}_1$ and $\vec{\lambda}_3$ only, since $\vec{\lambda}_2$ is negligibly small. In a low speed range, $\vec{\lambda}_1$ will not be orthogonal to the back emf. The vector $\vec{\lambda}_3$ drives the vector $\vec{\lambda}_1$ to the correct position. Re-writing Equation (39) as:

$$\vec{\lambda}_3 = \frac{1}{\omega_e(\sqrt{1 + (\omega_e T_c)^2})} \angle(\phi - 90^o) \vec{E}^{s*}_{qdr} \tag{50}$$

and letting

$$\vec{E}^s_{qdr} = \vec{E}^{s*}_{qdr} \tag{51}$$

$\vec{\lambda}^s_{qdr}$ can be written:

$$\vec{\lambda}^s_{qdr} = |\vec{\mu}| \left(T_c \angle\phi + \frac{1}{\omega_e} \angle(\phi - 90^o) \right) \vec{E}^s_{qdr} \tag{52}$$

Examining Equation (52), $\vec{\lambda}_3$ adds the necessary amount of phase to make the back emf and flux orthongonal in a low speed range, and thus is the *compensating* component of the flux estimator.

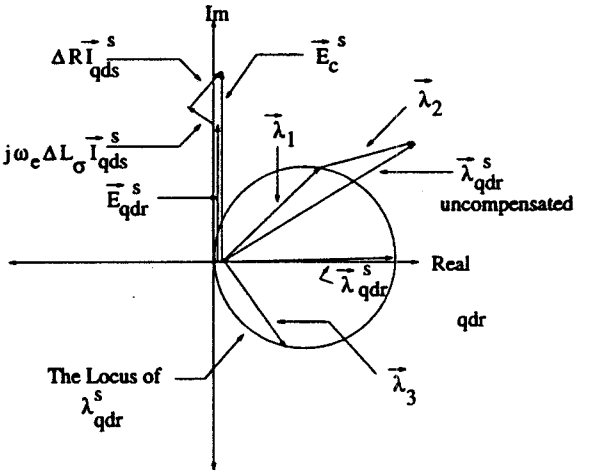

Figure 4: Phasor Diagram of Flux Estimator

A phasor diagram was constructed in Figure 4 to graphically illustrate how the components of the flux estimator are related. At low speeds, $\vec{\lambda}_1$ is not sufficiently shifted to be orthongonal to $\vec{E}^s_c$, such that the addition of $\vec{\lambda}_3$ will bring $\vec{\lambda}_1$ to its correct position. Also, as λ_2 approaches to zero, the sum of $\vec{\lambda}_2$ and $\vec{\lambda}_1$ approaches $\vec{\lambda}_1$, and the phase error due to the resistive parameters is reduced to a low level. Conversely, at high speeds $\vec{\lambda}_1$ is orthogonal to $\vec{E}^s_{qdr}$ and the magnitude of $\vec{\lambda}_3$ is quite small. In essence, the phase contribution of $\vec{\lambda}_3$ to $\vec{\lambda}_1$ is naturally reduced in a high speed range due to the low pass filter.

III. Computer Simulation

A computer simulation was conducted of the system shown in Figure 5 to investigate the performance of the estimator. The machine simulated has specifications listed in Table 1.

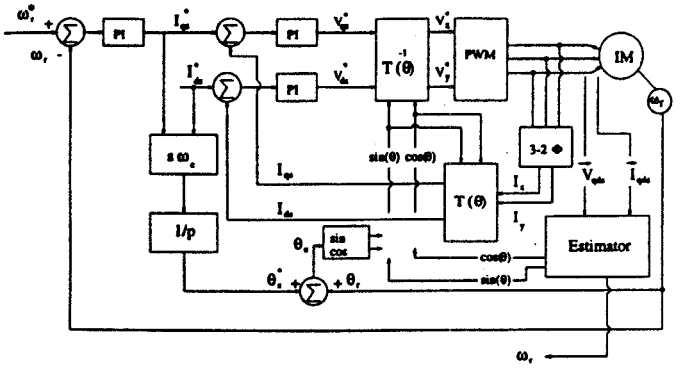

Figure 5: Indirect Field Oriented System

A step speed command of 800 rpm was given for the system shown in Figure 5. The encoder was used with the current sensors to provide the necessary feedback signals. The phase current i_a and electromagnetic torque T_e are shown in Figure 6, while the real and estimated values of $sin(\theta)$ and $cos(\theta)$ are shown in Figure 7. The real and estimated rotor speed are shown in Figure 8.

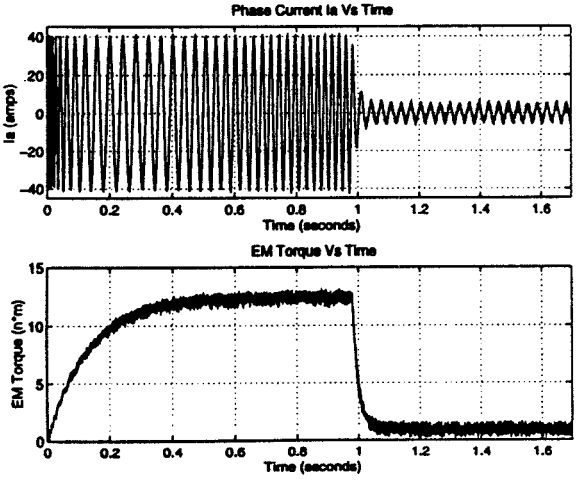

Figure 6: Phase Current and EM Torque

Examining Figures 7 and 8, the estimated values closely match the real values, demonstrating the effectiveness of the estimation algorithm.

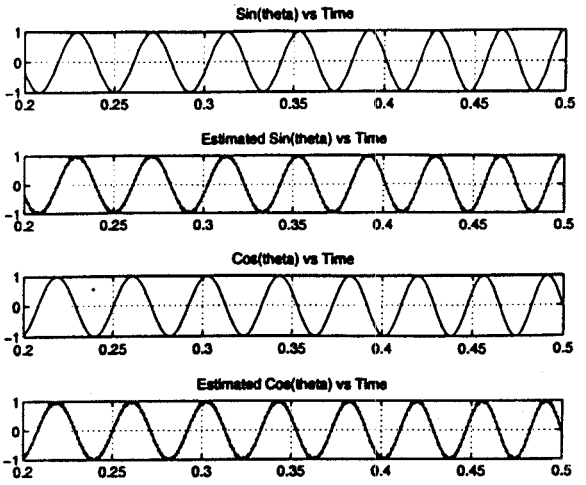

Figure 7: Real and Estimated $\sin(\theta)$ and $\cos(\theta)$

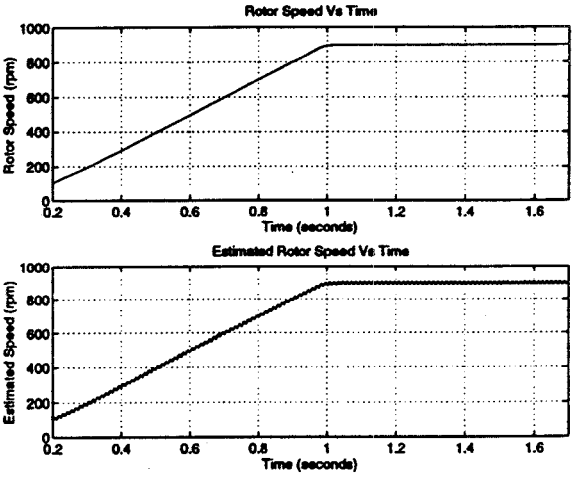

Figure 8: Command and Real Speed

IV. Laboratory Results

The system of Figure 5 was implemented with a DSP56001 to test the accuracy of the estimated angular waveforms. Figure 9 shows the real and estimated waveforms of $sin(\theta)$ and $cos(\theta)$. The top waveform is the real $sin(\theta)$, the second is the estimated $sin(\theta)$, the third waveform is the real $cos(\theta)$, and the estimated $cos(\theta)$ is the final waveform. Again, the current sensors and encoder provide feedback information, i.e. the estimated values are not used as feedback signals.

Examining Figure 9, the estimated values for both $sin(\theta)$ and $cos(\theta)$ closely match the real values. An estimate of rotor speed is now possible using equations (31), (33), and (34). However, elimination of noise introduced by (33) must occur before a clean

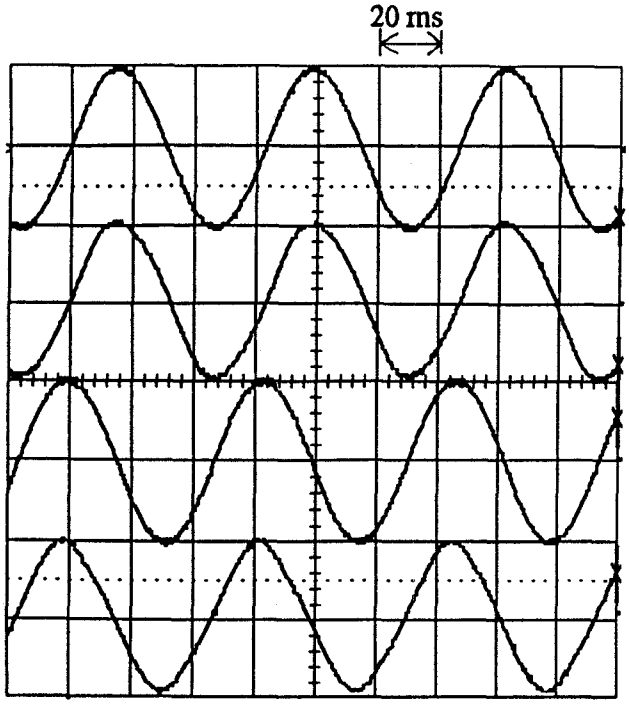

Figure 9: Real and Estimated $\sin(\theta)$ and $\cos(\theta)$

rotor speed estimate is produced.

Table1

220 Volts	15 Amps	5 HP
$L_\sigma = 4$ mH	M = 35.2 mH	1800 rpm
$R_s = 1.1\,\Omega$	$R_r = .2696\,\Omega$	4 poles

V. Conclusions

A physical approach is presented for a position sensorless, field oriented induction machine drive. The key issue in a position sensorless drive is to observe the rotor flux correctly. Then the rotor speed can be calculated accurately. For the physical approach, the rotor flux is estimated accurately by making the rotor flux and back emf orthogonal even in a low speed range and subject to parameter variations. The algorithm simplicity is an attractive feature for implementation on a DSP real time control system.

The laboratory implementation results are promising. Several key issues remain to be addressed regarding the performance of the estimator. These issues include producing a noise free rotor speed estimated, and any additional steps such as filtering to aid in estimating the rotor speed. Final laboratory results will be presented in the near future.

VI. References

[1] T. Ohtani, N. Takada, and K. Tanaka, "Vector Control of Induction Motor Without Shaft Encoder," in *Proceedings of the IEEE-IAS Annual Conference,* 1989, pages 500-507.

[2] H.Tajima, Y. Hori, "Speed Sensorless Field-Orientation Control of the Induction Machine," *IEEE-IAS Transactions,* Vol. 29, No. 1, pages 175-180, January-February 1993.

[3] Kubota, H., Matsuse, K., and Nakano, T., "DSP-Based Speed Adaptive Flux Observer of Induction Motor," *IEEE-IAS Transactions,* Vol. 29,No. 2, pages 344-348, March-April 1993.

[4] X. Xu, R. De Doncker, and D. Novotny, "Implementation of Direct Stator Flux Orientation Control on a Versatile DSP Based System," *Proceedings of the IEEE-IAS Annual Conference,"* 1990, pages 404-409.

[5] X. Xu, and D. Novotny, "Selection of the Flux Reference for Induction Machine Drives in the Field Weakening Region," *IEEE-IAS Transactions,* Volume 28, No. 6, pages 1353-1358, November/December 1992.

[6] F.Z. Peng, and T. Fukao, "Robust Speed Identification for Speed Sensorless Vector Control of Induction Motors," *Proceedings of the IEEE-IAS Annual Conference,* 1993, pages 419-426.

[7] P.L. Jansen, R.D. Lorenz, and D.W. Novotny, "Observer-Based Field Orientation Analysis and Comparison of Alternative Methods," *Proceedings of the IEEE-IAS Annual Conference,* 1993, pages 536-543.

[8] C. J. Bonanno, L. Xu, and X. Xu, "Robust, Parameter Insensitive Position Sensorless Field Orientation Control of the Induction Machine," *Proceedings of IEEE-PESC,* 1994, pages 752-757.

[9] W. Cheng, C. J. Bonanno, and L. Xu, "A General Purpose, Flexible DSP56001 Development System for Motion Control Applications," *1994 ICSPAT Conference,* Dallas, Texas.